Materials Chemistry and Physics 125 (2011) 887–894

Contents lists available at ScienceDirect

Materials Chemistry and Physics

journal homepage: www.elsevier.com/locate/matchemphys

First principles predictions on mechanical and physical properties of HoX (X = As, P)

C. Çoban [a,*], K. Çolakoğlu [b], Y.Ö. Çiftçi [b]

[a] Balıkesir University, Department of Physics, 10145 Çağış, Balıkesir, Turkey
[b] Gazi University, Department of Physics, Teknikokullar, 06500 Ankara, Turkey

ARTICLE INFO

Article history:
Received 18 May 2009
Received in revised form
11 September 2010
Accepted 19 September 2010

Keywords:
HoAs and HoP
Elastic properties
Lattice dynamics
Thermodynamic properties

ABSTRACT

In this study, the calculated results of the structural, electronic, elastic, lattice dynamic, and thermodynamic properties of HoX (X = As, P) in rocksalt structure (B1) are presented. Ab initio calculations were performed based on density-functional theory using the Vienna Ab initio Simulation Package (VASP). Calculated structural parameters, such as the lattice constant, bulk modulus and its pressure derivative, cohesive energy, second-order elastic constants, electronic band structures and related total and partial density of states, Zener anisotropy factor, Poisson's ratio, Young's modulus, and isotropic shear modulus are presented. In order to gain further information, we investigated the pressure and temperature dependent behavior of the volume, bulk modulus, thermal expansion coefficient, heat capacity, entropy, Debye temperature, and Grüneisen parameter over a pressure range of 0–32 GPa and a wide temperature range of 0–2000 K. The phonon frequencies and one-phonon density of states are also presented.

1. Introduction

In recent years, the monopnictides and monochalcogenides of the rare-earth elements with rocksalt structure (B1) have aroused intensive interest due to the presence of strongly correlated f-electrons in them. Under pressure, the nature of f-electrons of these compounds can be changed from localized to itinerant leading to significant changes in physical and chemical properties [1]. These unusual structural, electronic, and high-pressure properties make them candidates for advanced industrial applications which include alloys, catalysts, ceramics, glass, magnetics, nuclear, and phosphors. For these applications, they provide unique physical properties which cannot be achieved with other materials. Rare-earth pnictides are typically low carrier, strongly correlated systems [2] and they also show dense kondo behavior, heavy fermion state [3–7]. The term heavy fermions has been coined to describe kondo lattices which have specific heat coefficients greater than 400 mJ mol^{-1} K^2 [8]. Holmium arsenide and holmium phosphide (HoX (X = As, P)) are the members of rare-earth compounds and crystallize in B1 structure (Ho: 0, 0, 0; X = As, P: 1/2, 1/2, 1/2; space group $Fm\bar{3}m$ (2 2 5)).

A few experimental studies of HoAs and HoP have been reported in the literature. Shirotani et al. [9] have measured the X-ray diffraction pattern by using synchrotron radiation and investigated pressure-induced phase transitions of the heavier LnAs (Ln = Pr, Nd, Sm, Gd, Dy and Ho) compounds. Fischer et al. [10] have performed neutron scattering experiments on HoP to obtain the phase diagrams.

So far, to our knowledge, the electronic, elastic, lattice dynamic, and thermodynamic properties of HoX (X = As, P) have not been studied systematically. Therefore, we calculated and presented a set of physical parameters of these compounds in B1 structure such as optimized lattice parameters (a), bulk modulus (B), pressure derivative of bulk modulus (B'), cohesive energy (E_{coh}), electronic band structures and related total and partial density of states (DOS and PDOS). In addition to this, second-order elastic constants (C_{ij}), Zener anisotropy factor (A), Poisson's ratio (ν), Young's modulus (E), and isotropic shear modulus (G) were also obtained. Particularly, our research focuses on mechanical, lattice dynamic, and thermodynamic properties. The pressure and temperature dependence of the volume, bulk modulus, thermal expansion coefficient, heat capacities, entropy, Debye temperature, and Grüneisen parameter were also investigated.

2. Method of calculation

All the parameters were computed with the Vienna Ab initio Simulation Package (VASP) [11–15]. It performs an iterative solution of the generalized Kohn–Sham equations of density-functional theory, based on the minimization of the norm of the residual vector to each eigenstate and an efficient charge density mixing [16]. The gradient-corrected functionals in the form of

* Corresponding author. Tel.: +90 266 6121278/1206; fax: +90 266 6121215.
E-mail address: cansucoban@yahoo.com (C. Çoban).

0254-0584/$ – see front matter © 2010 Elsevier B.V. All rights reserved.
doi:10.1016/j.matchemphys.2010.09.024

the generalized-gradient approximation (GGA) by Perdew and Wang [17,18] were chosen. The projector-augmented wave (PAW) method developed by Blöchl [19] and implemented within VASP was used in our calculations to describe the interactions between ions and electrons. PAW method is an extension of augmented wave methods and the pseudopotential approach [19]. It is built on projector functions that allow to use 'pseudo' wave functions instead of the complicated wave functions, which are easier to treat computationally. In pseudopotential approach, only valence electrons are taken into account in the calculation. The interactions between ions and electrons are described by a pseudopotential without norm constraint. The potpaw_GGA pseudopotential was used for these compounds (HoX (X = As, P)). The distributed PAW potentials for VASP have been generated by G. Kresse following the procedure discussed in Ref. [20]. All the results presented below were obtained by using a plane wave basis with an energy cutoff of 500 eV. The $12 \times 12 \times 12$ Monkhorst and Pack scheme [21] of k-points were used for the sampling of the Brillouin zone.

The present GGA phonon frequencies of HoAs and HoP compounds were calculated by the PHON program [22] using the forces based on the VASP package. The PHON code generates all elements of the force constant matrix. It calculates phonon frequencies and one-phonon density of states (DOS) using the "Small Displacement Method" described in Ref. [23] which is a similar procedure as described in Ref. [24]. The $2 \times 2 \times 2$ cubic supercell of 48 atoms was constructed by using supercell generation method implemented in PHON program for calculating the phonon dispersion curves and one-phonon density of state in high symmetry directions for HoX (X = As, P) compounds.

The quasi-harmonic Debye model [25] was applied to calculate thermodynamic properties of HoX (X = As, P) compounds by using GIBBS program [25]. The GIBBS program is used to investigate isothermal–isobaric thermodynamics of solids from energy curves using a quasi-harmonic Debye model. In this model, the non-equilibrium Gibbs function $G^*(V; P, T)$ is defined as [26]:

$$G^*(V; P, T) = E(V) + PV + A_{vib}\left[\Theta(V); T\right] \tag{1}$$

where $E(V)$ is the total energy for per unit cell of HoX (X = As, P), PV is the constant hydrostatic pressure condition, $\Theta(V)$ is the Debye temperature and A_{vib} is the vibrational Helmholtz free energy. The vibrational contribution A_{vib} is given as [27–31]:

$$A_{vib}(\Theta, T) = nkT\left[\frac{9\Theta}{8T} + 3\ln(1 - e^{-\Theta/T}) - D(\Theta/T)\right] \tag{2}$$

where n is the number of atoms per formula unit, $D(\Theta/T)$ represents the Debye integral. The Debye temperature, Θ, is expressed as [31]:

$$\Theta = \frac{\hbar}{k}\left[6\pi^2 V^{1/2} n\right]^{1/3} f(\sigma)\sqrt{\frac{B_s}{M}} \tag{3}$$

where M is the molecular mass per unit cell and B_s is the adiabatic bulk modulus that measures the compressibility of the crystal, which is defined by [25]:

$$B_s \approx B(V) = V\frac{d^2E(V)}{dV^2}, \tag{4}$$

$f(\sigma)$ is given by [28,29]:

$$f(\sigma) = \left\{3\left[2\left(\frac{2}{3}\frac{1+\sigma}{1-2\sigma}\right)^{3/2} + \left(\frac{1}{3}\frac{1+\sigma}{1-\sigma}\right)^{3/2}\right]^{-1}\right\}^{1/3}, \tag{5}$$

where σ is Poisson's ratio. By solving the following equation with respect to V:

$$\left[\frac{\partial G^*(V; P, T)}{\partial V}\right]_{P,T} = 0, \tag{6}$$

the thermal equation of state (EOS) $V(P, T)$ can be obtained. The thermal expansion coefficient, α, can be expressed as [25]:

$$\alpha = \frac{\gamma C_V}{B_T V}, \tag{7}$$

where B_T is isothermal bulk modulus, C_V is the heat capacity at constant volume, and γ is the Grüneisen parameter which are given by [25]:

$$B_T(P, T) = V\left(\frac{\partial^2 G^*(V; P, T)}{\partial V^2}\right)_{P,T}, \tag{8}$$

$$C_V = 3nk\left[4D(\Theta/T) - \frac{3\Theta/T}{e^{\theta/T} - 1}\right], \tag{9}$$

$$\gamma = -\frac{d\ln\Theta(V)}{d\ln V}. \tag{10}$$

The other thermodynamic quantities, e.g., heat capacity at constant pressure C_P, entropy S, can be calculated by applying the following relations [25]:

$$C_P = C_V(1 + \alpha\gamma T), \tag{11}$$

$$S = nk\left[4D\left(\frac{\Theta}{T}\right) - 3\ln(1 - e^{-\Theta/T})\right]. \tag{12}$$

3. Results and discussion

3.1. Structural and electronic properties

The equilibrium lattice constant, bulk modulus, and its pressure derivative were computed by minimizing the total energy for B1 structure of the HoX (X = As, P) crystals calculated at different volumes by means of Murnaghan's equation of state [32]. Optimized lattice constants, presented in Table 1, are found to be 5.80 and 5.64 Å for HoAs and HoP, respectively. They are in good agreement with the experimental data taken from Ref. [7]. Calculated value of bulk modulus and its pressure derivative are also presented in Table 1 for B1 structure. The previous experimental or other theoretical results are not available for the comparison with the present values of bulk modulus and its pressure derivative.

The cohesive energy is a measure of the strength of the forces which is calculated by using the Eq. (13) for B1 structure of HoAs and HoP:

$$E_{coh}^{AB} = [E_{atom}^{A} + E_{atom}^{B} - E_{total}^{AB}] \tag{13}$$

where E_{total}^{AB} is the total energy of the HoAs and HoP at equilibrium lattice constant, E_{atom}^{A} and E_{atom}^{B} are the atomic energies of the pure constituents. The computed cohesive energies, listed in Table 1, are found to be 6.37, and 7.20 eV/atom for B1 structure of HoAs and HoP compounds, respectively. The previous results are not existing in the literature for the comparison.

We also computed the electronic band structures of HoX (X = As, P) for B1 phases along the high symmetry directions using the calculated equilibrium lattice constant (Fig. 1). It can be seen from Fig. 1 that, no band gap exists for B1 phases of these compounds. Therefore, these structures exhibit nearly a semi-metallic character. The total DOS and PDOS corresponding to the present band structures are also presented in Fig. 1. The structure is metallic because of the presence of finite DOS at the Fermi level (E_F) as in Ref. [33], and absence of energy gap in DOS profiles which conforms the metallic nature of the compounds. In PDOS profiles for HoAs, the lowest valence bands, which have occurred between about −24 eV and −23 eV below the Fermi level (E_F), are essentially dominated by Ho-p states. The other valence bands that between about −11.2 eV and −9.2 eV are dominated by Ho-d states. The s, p, and d states of As atoms are also minor contributing to the lowest valence band

Table 1
Calculated lattice constant (a), bulk modulus (B), pressure derivative of bulk modulus (B'), cohesive energy (E_{coh}) for B1 structure of HoX (X = As, P).

Material	Reference	a (Å)	B (GPa)	B'	E_{coh} (eV/atom)
HoAs (B1)	Present (GGA)	5.80	76.75	3.88	6.37
	Experiment[a]	5.76			
HoP (B1)	Present (GGA)	5.64	86.57	3.70	7.20
	Experiment[a]	5.615			

[a] Ref. [7].

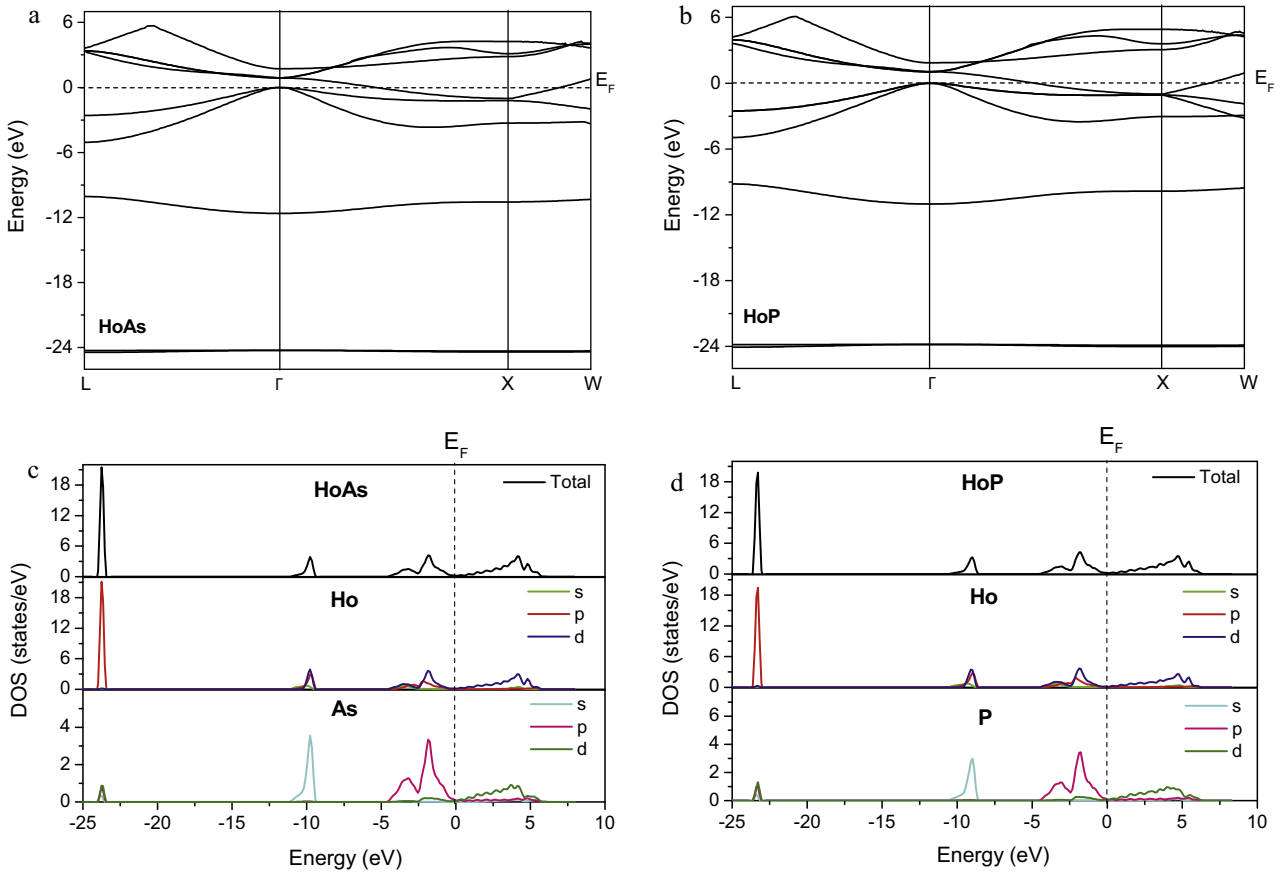

Fig. 1. Calculated electronic band structures, total density of states and partial density of states for B1 phase of (a) HoAs, (b) HoP, (c) HoAs, and (d) HoP.

and s state of As atoms are major contributing to the valance band between −11.2 eV and −9.2 eV. The last valence bands are essentially dominated by Ho-d sates between about −2.5 eV and 0 eV and by As-p states between about −4.5 eV and −2.5 eV. The conduction band consists of Ho-s, Ho-p, Ho-d, As-s, As-p, and As-d states which is dominated by Ho-d states. Therefore, it can be concluded that the electronic bands around the Fermi level (E_F) are formed mainly by Ho-d states of HoX (X = As, P), and these delocalized states are responsible for metallic-like Ho–Ho bonds. The similar situations were observed for HoP in the PDOS profile. The previous experimental or other theoretical works are not available to compare with our results.

3.2. Elastic properties

The elastic constants are important characteristic parameters of solids. The investigation of them is essential to understand many of their physical properties such as elasticity, mechanical stability, stiffness of materials, and concerning the nature of the forces operating in solids. Here, the second-order elastic constants, presented in Table 2, were calculated using the "volume-conserving" technique [34,35] as we have done recently for other transition-metal pnictides (LaAs, LaP) [36]. The known mechanical stability conditions for cubic compounds led to the restrictions on the elastic constants known as $C_{11}-C_{12}>0$, $C_{11}>0$, $C_{44}>0$, $C_{11}+2C_{12}>0$. Our calculated results for elastic constants, presented in Table 2, satisfy these stability conditions and the other cubic stability condition, $C_{12}<B<C_{11}$ for HoAs and HoP. Unfortunately, to our knowledge, there is no available data of elastic parameters to compare with the present results.

The elastic properties such as the Zener anisotropy factor (A), Poisson's ratio (ν), and Young's modulus (E) are measured for polycrystalline materials when their hardness is being investigated. These are calculated in terms of computed data using the following

Table 2
Elastic constants (in GPa), the calculated Zener anisotropy factor (A), Poisson's ratio (ν), Young's modulus (E) (in GPa), and isotropic shear modulus (G) (in GPa) for HoX (X = As, P) in B1 structure.

Material	Reference	C_{11}	C_{12}	C_{44}	A	ν	E	G
HoAs (B1)	Present	114.27	57.99	10.68	0.38	0.40	44.71	15.93
HoP (B1)	Present	126.89	66.41	12.71	0.42	0.40	50.85	18.13

relations [37,38]:

$$A = \frac{2C_{44}}{C_{11} - C_{12}}, \tag{14}$$

$$\nu = \frac{1}{2}\left[\frac{(B - (2/3)G)}{(B + (1/3)G)}\right], \tag{15}$$

and

$$E = \frac{9GB}{G + 3B} \tag{16}$$

where $G = (G_V + G_R)/2$ is the isotropic shear modulus, G_V is Voigt's shear modulus corresponding to the upper bound of G values, and G_R is Reuss's shear modulus corresponding to the lower bound of G values; they can be written as: $G_V = (C_{11} - C_{12} + 3C_{44})/5$, and $5/G_R = 4/(C_{11} - C_{12}) + 3/C_{44}$.

The calculated Zener anisotropy factor, A, Poisson's ratio, ν, Young's modulus, E, and isotropic shear modulus, G, for HoX (X = As, P) are also presented in Table 2.

The measure of the anisotropy in a solid is represented by the Zener anisotropy factor. For the values of A smaller or greater than 1, it is a measure of the degree of elastic anisotropy. If A takes the value of 1, the material is called completely isotropic. The calculated Zener anisotropy factors for HoX (X = As, P) are smaller than 1 which indicates that these compounds are not elastically isotropic.

The Young's modulus, E, and Poisson's ratio, ν, are very important properties for industrial applications. The Young's modulus, E, the ratio of the tensile stress to the corresponding tensile strain, is required to provide information about the measure of the stiffness of the solids. The present values of Young's moduli increase from As to P, which points out that the stiffness of the materials also increases from As to P.

The lower limit and upper limit of Poisson's ratio, ν, are given 0.25 and 0.5 for central forces in solids, respectively [39]. Besides, it is small for covalent materials ($\nu = 0.1$) and grows essentially

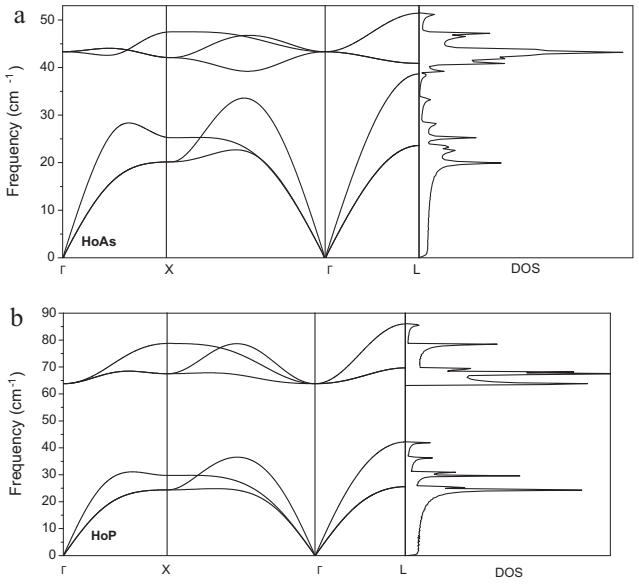

Fig. 2. Calculated phonon dispersion curves and one-phonon density of states for (a) HoAs and (b) HoP in B1 structure.

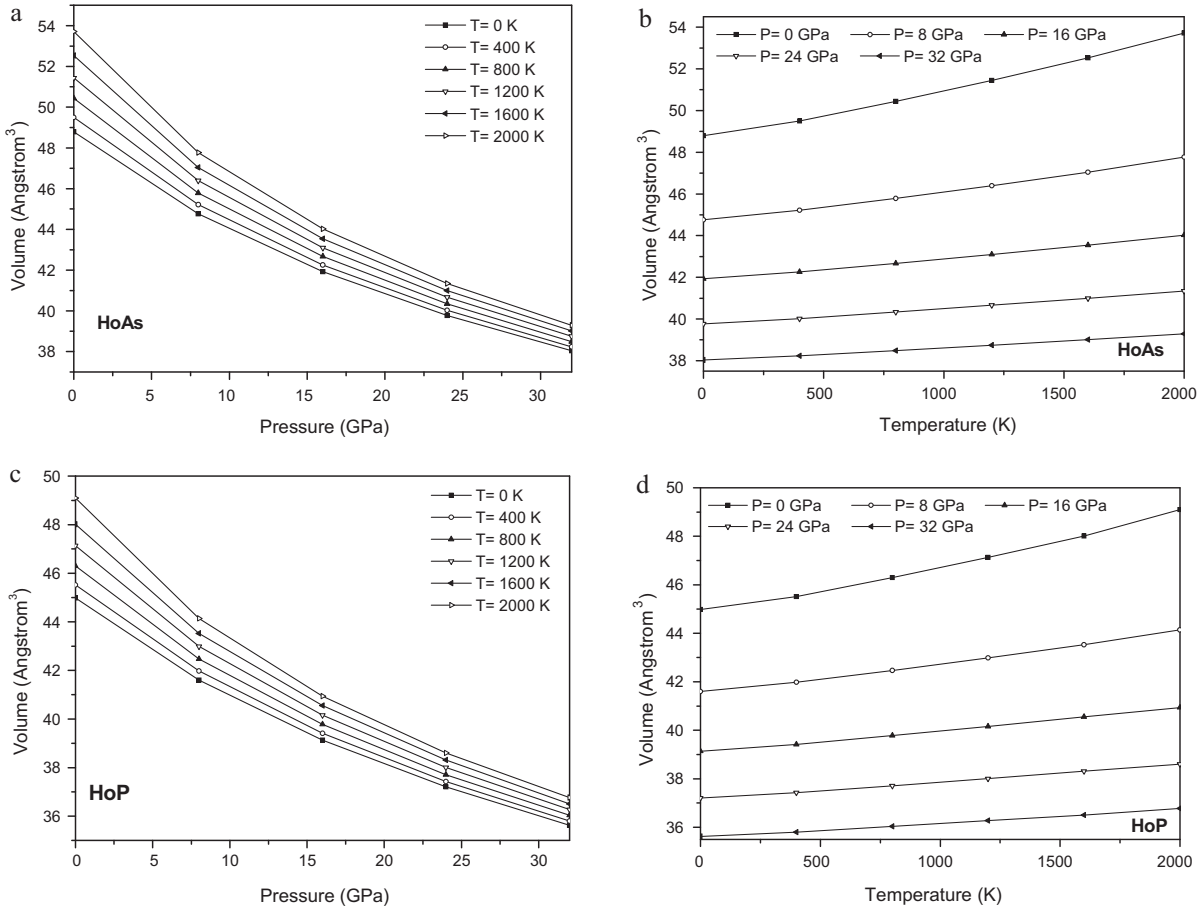

Fig. 3. The pressure and temperature dependence of the volume of (a), (b) HoAs and (c), (d) HoP.

for ionic materials [40]. Calculated values are equal to 0.40 which shows that the interatomic forces in the HoX (X = As, P) are predominantly central forces and a considerable ionic contribution in intra-atomic bonding takes place for this phase.

It is known that, the hardness of a compound can be measured using the isotropic shear modulus and bulk modulus. The bulk modulus is a measure of resistance to volume change by applied pressure, whereas the shear modulus is a measure of resistance to reversible deformations upon shear stress [41]. Therefore, by using the isotropic shear modulus, G, the hardness of a material can be determined more accurately than by using the bulk modulus. The calculated G are 15.93 and 18.13 GPa for HoX (X = As, P), respectively. Thus, these are highly compressible compounds. According to criterion [42,43], if the B/G ratio is smaller than 1.75, the material is brittle, otherwise it behaves in ductile manner. Calculated values of the B/G are found to be 4.82 and 4.77 for HoAs and HoP, respectively. Since they are greater than 1.75, these materials will not behave in a brittle manner.

3.3. Lattice dynamic properties

The phonon dispersion curves and one-phonon DOS without LO/TO splitting were calculated for B1 phase of all compounds and illustrated in Fig. 2. The experimental and other theoretical results on the lattice dynamics of these compounds in the literature do not exist for the comparison with the present data. It is seen that the shape of the dispersion curves changes depending on the mass difference between pnictide ions. Although a clear gap (about 22 cm^{-1}) between the acoustic and optical branches is formed (observed) for HoP compound, it is smaller (about 2.3 cm^{-1}) for HoAs. In addition to this, the soft modes are not observed for considered phase, i.e., the B1 is clearly a stable structure. The maximum values of the phonon frequencies for acoustic branches decrease as one goes from P to As atom.

3.4. Thermodynamic properties

The thermodynamic properties of HoX (X = As, P) compounds were predicted using the quasi-harmonic Debye model up to 2000 K. Fig. 3(a)–(d) shows the pressure and temperature dependence of the volume of HoAs and HoP, respectively. For all temperatures, the volume exhibits decreasing trend with increasing pressure. Due to the stronger atomic interactions in the interlayer, these changes can be occured. For both compounds, the volume increases gradually with the increase of the temperature at pressures higher than 0 GPa. At 0 GPa, the volume exhibits rapid increase than at higher pressures.

We investigated the pressure dependence of bulk modulus, B, with the temperature varying from 0 to 2000 K by applying the quasi-harmonic Debye model described above. The temperature dependent behavior of the bulk modulus, B, was plotted in Fig. 4. Relationships between bulk modulus, B, and pressure, P, at different temperatures were also plotted in Fig. 4. From Fig. 4, the bulk modulus, B, decreases gradually as T increases, which indicates that the cell volume undergoes gradual changes. It is clearly seen from Fig. 4 that, at a given temperature, the bulk modulus, B, increases with increasing pressure vividly. We can say that, the effect of increasing pressure is the same as the decreasing temperature on HoAs and HoP.

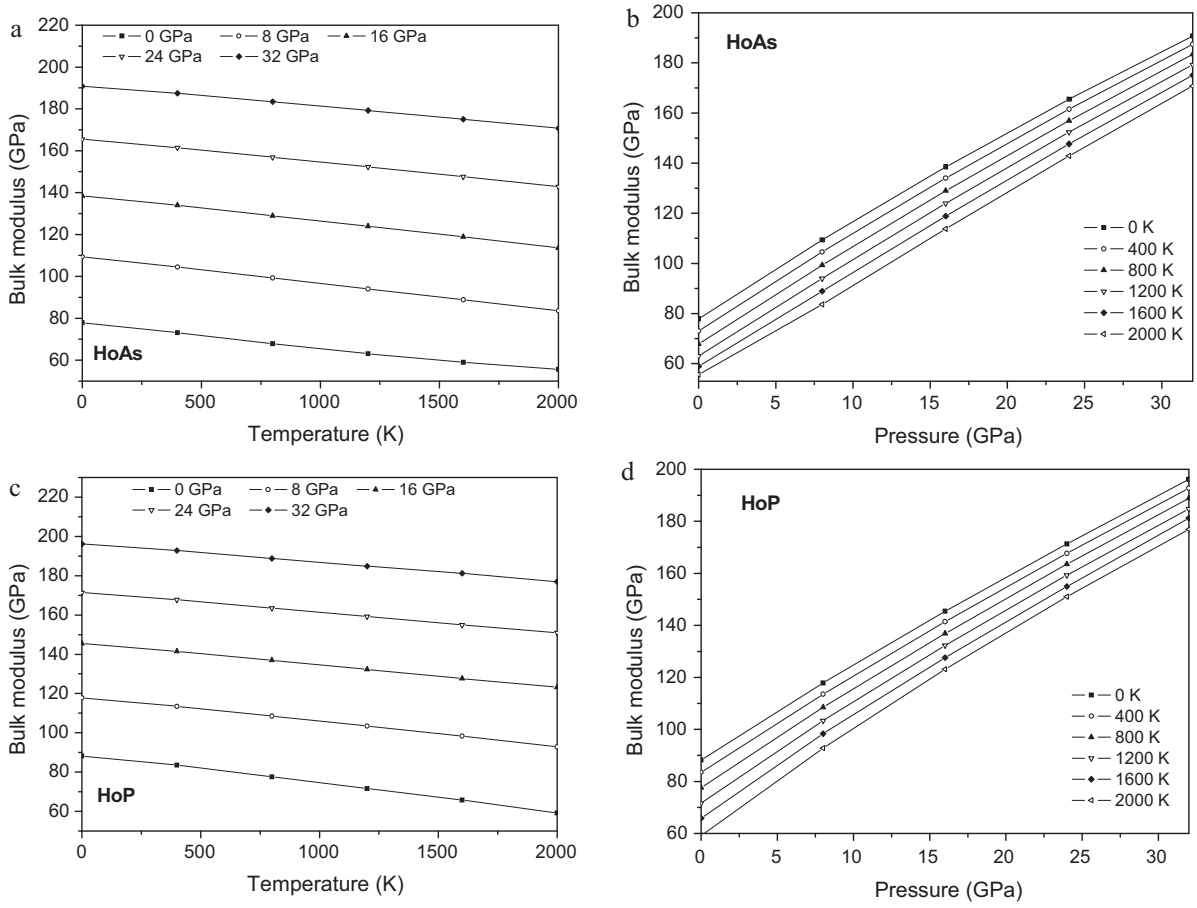

Fig. 4. The temperature and pressure dependence of bulk modulus of (a), (b) HoAs and (c), (d) HoP.

Table 3
Summary of thermal parameters for HoX (X = As, P).

Material	Reference	$(dB/dT)_{p=0\,GPa}$ (for $T = 400$ K) (GPa K^{-1})	α_T (K^{-1}) = $a + bT$ ($P = 0$ GPa)		$(d\alpha/dP)_{T=400\,K}$ ($\times 10^{-8}$) (GPa^{-1} K^{-1})
			a ($\times 10^{-5}$)	b ($\times 10^{-8}$)	
HoAs (B1)	Present	−0.0126	2.2455	4.4736	−4.7150
HoP (B1)	Present	−0.0132	1.8544	4.0403	−2.4596

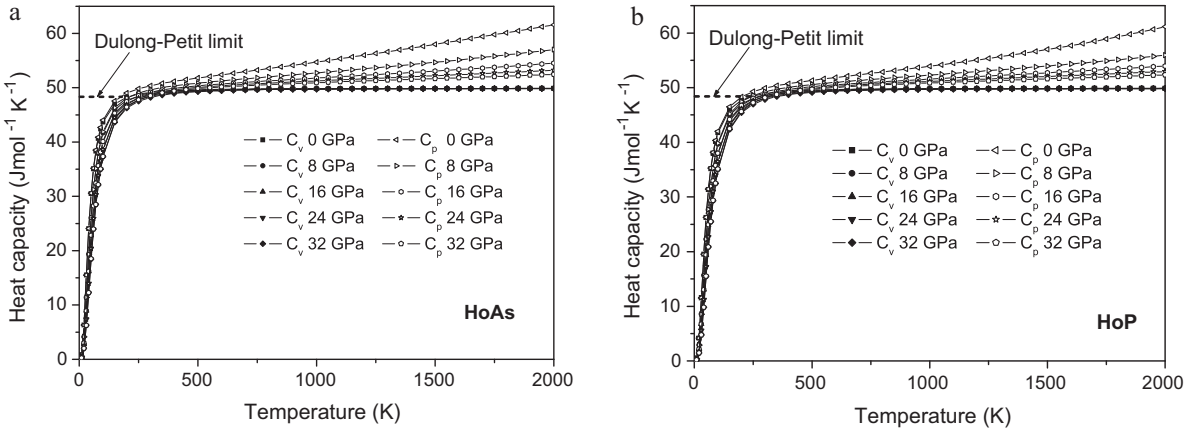

Fig. 5. The variations of heat capacities C_V and C_P with the temperature for (a) HoAs and (b) HoP.

At $P = 0$, by fitting the B–T data points to third-order polynomial (see Ref. [44]), for $T = 400$ K, the temperature derivative of the B, listed in Table 3, is found to be −0.0126 and −0.0132 GPa K^{-1} for HoX (X = As, P), respectively.

Calculated relationships between heat capacities at constant volume C_V, at constant pressure C_P and temperatures at different pressures were plotted in Fig. 5. As we can see from Fig. 5 that, when $T < 250$ K C_V increases rapidly with temperature at a given pressure and decreases with pressure at a given temperature. Due to the use of anharmonic approximation of the Debye model, the heat capacities C_V and C_P exhibit powerfull dependency on temperature T and pressure P for the temperature smaller than 250 K. For the temperatures higher than 250 K, the influence of anharmonicity on heat capacity C_V is controlled. It is less than on C_P. At high temperatures, C_P increases linearly whereas the C_V approaches the Dulong–Petit limit ($C_V(T) \sim 3R$) as shown in Fig. 5. This indicates that the atomic interactions in HoAs and HoP compounds especially occur at low temperatures. At all temperatures, the C_V of HoAs yields larger values compared to that of HoP, i.e., at 300 K (at about room temperature), the C_V is found to be 49.16 and 48.90 J mol^{-1} K^{-1} for HoAs and HoP, respectively.

The variations of entropy, S, with the temperature at different pressures for HoX (X = As, P) compounds are presented in Fig. 6. Obviously, entropy increases with increasing temperature but it decreases with the pressure.

The variations of thermal expansion coefficient, α, with different temperatures at different pressures were plotted in Fig. 7. As can be seen in this figure, at low temperatures ($T < 250$ K) α increases rapidly and at high temperatures this trend is not exhibited. Particularly, at high temperatures ($T > 250$ K), it decreases with increasing pressure. It is worthwhile to note that as the pressure increases, the increase of α with temperature becomes smaller.

The volumetric thermal expansion $\alpha(0,T)$ at atmospheric pressure, commonly represented by $\alpha(0,T) = a + bT - c/T^2$ for T in Kelvin (see Refs. [45,46]). Thus, by fitting the α–T data points to second order polynomial, the a and b values are found to be, 2.2455×10^{-5}, 4.4736×10^{-8} and 1.8544×10^{-5}, 4.0403×10^{-8} for HoX (X = As, P), respectively. The term of c/T^2 is ignored as well as higher order terms of the bulk modulus temperature derivative such as third-order derivative of bulk modulus. At 400 K, the pressure derivative of the thermal expansion coefficient is calculated to be -4.7150×10^{-8} and -2.4596×10^{-8} GPa^{-1} K^{-1} for

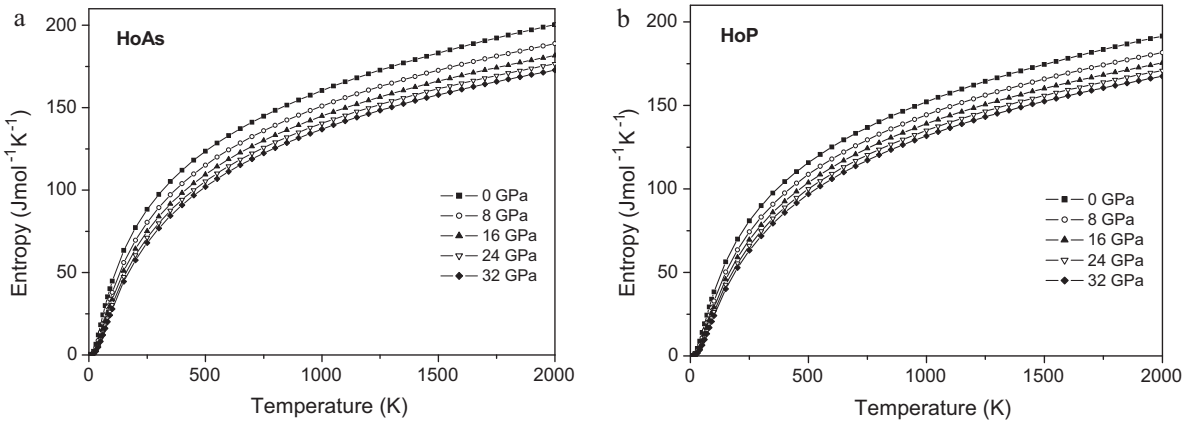

Fig. 6. Temperature dependence of entropy for (a) HoAs and (b) HoP.

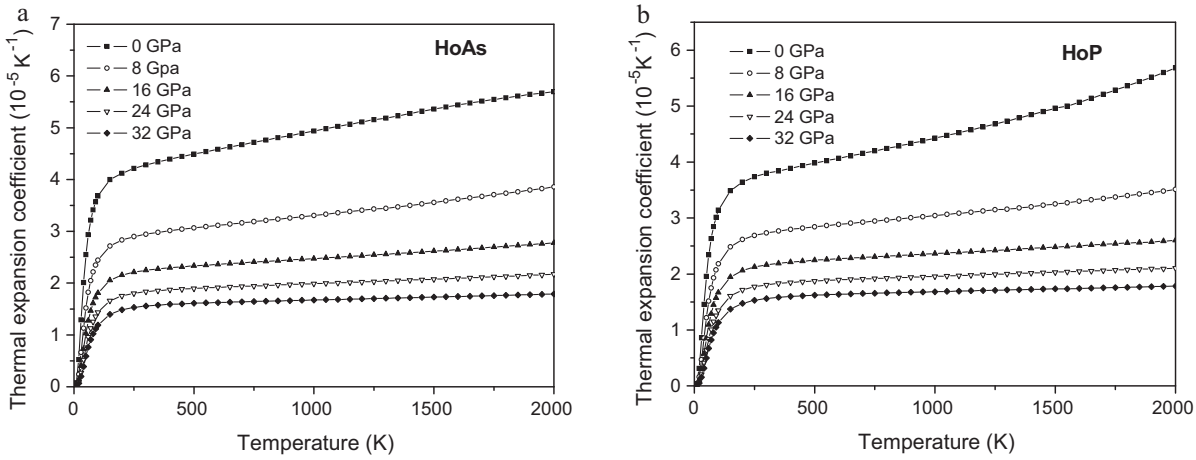

Fig. 7. The thermal expansion coefficient versus temperature curves for (a) HoAs and (b) HoP.

Table 4
The variations of calculated Debye temperature Θ (K) and the Grüneisen parameter γ with different temperatures and pressures for HoX (X = As, P) compounds.

T (K)	Material										
	HoAs (B1)						HoP (B1)				
	P (GPa)										
		0	8	16	24	32	0	8	16	24	32
0	Θ	165.74	193.79	215.80	233.85	249.27	192.62	219.87	241.83	260.34	276.54
	γ	1.905	1.716	1.577	1.473	1.393	1.778	1.614	1.503	1.421	1.356
400	Θ	161.24	190.43	213.14	231.70	247.48	188.57	216.65	239.21	258.16	274.68
	γ	1.935	1.738	1.593	1.485	1.402	1.805	1.632	1.516	1.430	1.363
800	Θ	155.44	186.30	209.85	229.00	245.21	182.78	212.58	235.90	255.37	272.24
	γ	1.971	1.766	1.613	1.500	1.413	1.845	1.655	1.532	1.442	1.373
1200	Θ	149.46	181.95	206.48	226.24	242.90	176.80	208.30	232.49	252.49	269.72
	γ	2.005	1.796	1.634	1.516	1.425	1.888	1.680	1.548	1.455	1.383
1600	Θ	143.25	177.47	203.00	223.43	240.52	170.67	203.96	228.96	249.53	267.46
	γ	2.035	1.826	1.656	1.532	1.438	1.934	1.706	1.566	1.468	1.392
2000	Θ	136.88	172.53	199.36	220.53	238.09	163.33	199.10	225.56	246.82	264.70
	γ	2.056	1.860	1.680	1.549	1.451	1.992	1.736	1.584	1.480	1.403

HoAs and HoP, respectively. These parameters are also listed in Table 3.

Finally, Debye temperature, Θ, which is an important physical parameter, and Grüneisen parameter, γ, were calculated in quasi-harmonic approximation and the results are presented in Table 4 for both compounds. The Θ decreases as temperature increases, but increases as pressure increases. It is shown that, at constant temperature, the Debye temperature, Θ, increases almost linearly with the pressure. The Grüneisen parameter, γ, increases with temperature, but unlike Θ, it decreases with increasing pressure.

To our knowledge, there is no previous experimental or theoretical data related to presented thermodynamic properties to compare our calculated results.

4. Summary and conclusion

In summary, we performed ab initio calculations to obtain structural, electronic, elastic, lattice dynamic, and thermodynamic properties of HoX (X = As, P) compounds. The optimized lattice parameters are presented. Some of our results, such as bulk modulus (B), pressure derivative of bulk modulus (B'), the cohesive energy, (E_{coh}), band structures and related total and partial density of states (DOS and PDOS), second-order elastic constants (C_{ij}), Zener anisotropy factor (A), Poisson's ratio (ν), Young's modulus (E), isotropic shear modulus (G) were obtained and reported here for the B1 structures of these compounds for the first time, to our knowledge. The present lattice constants are in good aggrement with the previous work. Our results for elastic constants satisfy the traditional mechanical stability conditions. For the first time again, we analysed the behavior of volume and bulk modulus of HoAs and HoP over a pressure range of 0–32 GPa and a wide temperature range of 0–2000 K. It is found that, while the volume decreases with increasing pressure, the bulk modulus B increases monotonically with the increase of pressure. The temperature dependences of heat capacities C_V and C_P, entropy, S, and thermal expansion coefficient, α, at various pressures were investigated. Finally, Debye temperature, Θ, and Grüneisen parameter, γ, were calculated at different temperatures and pressures.

Acknowledgement

This work is supported by Gazi University Research-Project Unit under Project No.: 05/2008-16.

References

[1] N.V.C. Shekar, P.C.H. Sahu, J. Mater. Sci. 41 (2006) 3207.
[2] D.X. Li, Y. Haga, H. Shida, T. Suzuki, Y.S. Kwon, Phys. Rev. B 54 (1996) 10483.
[3] M. Yoshida, K. Koyama, T. Sakon, A. Ochiai, M. Motokawa, J. Phys. Soc. Jpn. 69 (2000) 3629.
[4] O. Vogt, K. Mattenberger, in: K.A. Gschneidner, L. Erying Jr. (Eds.), Handbook on the Physics and Chemistry of Rare Earths, 1979, North Holland, Amsterdam.
[5] T. Suzuki, Jpn. J. Appl. Phys. Ser. 8 (1993) 1131.
[6] T. Suzuki, Physica B 347 (1993) 186.
[7] F. Hulliger, in: K.A. Gschneidner, L. Eyring (Eds.), Handbook on the Physics and Chemistry of Rare Earths, vol. 4, 1979, North-Holland, Amsterdam, p. 153.

[8] G. Vaitheeswaran, V. Kanchana, M. Rajagopalan, J. Alloys Compd. 336 (2002) 46.
[9] I. Shirotani, K. Yamanashi, J. Hayashi, Y. Tanaka, N. Ishimatsu, O. Shimomura, T. Kikegawa, J. Phys.: Condens. Matter 13 (2001) 1939.
[10] P. Fischer, A. Furrer, E. Kaldis, D. Kim, J.K. Kjems, P.M. Levy, Phys. Rev. B 31 (1985) 456.
[11] G. Kresse, J. Hafner, Phys. Rev. B 47 (1993) 558.
[12] G. Kresse, J. Hafner, J. Phys.: Condens. Matter 6 (1994) 8245.
[13] G. Kresse, J. Hafner, Phys. Rev. B 49 (14) (1994) 251.
[14] G. Kresse, J. Furthmüller, Comput. Mater. Sci. 6 (1996) 15.
[15] G. Kresse, J. Furthmüller, Phys. Rev. B 54 (11) (1996) 169.
[16] T. Demuth, J. Hafner, L. Benco, H. Toulhoat, J. Phys. Chem. B 104 (2000) 4593.
[17] J.P. Perdew, Y. Wang, Phys. Rev. B 45 (13) (1992) 244.
[18] J.P. Perdew, J.A. Chevary, S.H. Vosko, K.A. Jackson, M.R. Pedersen, D.J. Singh, C. Fiolhais, Phys. Rev. B 46 (1992) 6671.
[19] P.E. Blöchl, Phys. Rev. B 50 (17) (1994) 953.
[20] G. Kresse, J. Joubert, Phys. Rev. B 59 (1999) 1758.
[21] H.J. Monkhorst, J.D. Pack, Phys. Rev. B 13 (1976) 5188.
[22] http://chianti.geol.ucl.ac.uk/~dario/, 1998.
[23] D. Alfè, G.D. Price, M.J. Gillan, Phys. Rev. B 64 (2001) 045123.
[24] G. Kresse, J. Furthmüller, J. Hafner, Europhys. Lett. 32 (1995) 729.
[25] M.A. Blanco, E. Francisco, V. Luaña, Comput. Phys. Commun. 158 (2004) 57.
[26] A.A. Maradudin, E.W. Montroll, G.H. Weiss, I.P. Ipatova, Theory of Lattice Dynamics in the Harmonic Approximation, Academic Press, New York, 1971.
[27] M.A. Blanco, A. Martín Pendás, E. Francisco, J.M. Recio, R. Franco, J. Mol. Struct. (Theochem.) 368 (1996) 245.
[28] E. Francisco, J.M. Recio, M.A. Blanco, A. Martín Pendás, J. Phys. Chem. 102 (1998) 1595.
[29] E. Francisco, M.A. Blanco, G. Sanjurjo, Phys. Rev. B 63 (2001) 094107.
[30] M. Flórez, J.M. Recio, E. Francisco, M.A. Blanco, A. Martín Pendás, Phys. Rev. B 66 (2002) 144112.
[31] M.A. Blanco, PhD thesis, Universidad de Oviedo, 1997, URL http://web.uniovi.es/qcg/mab/tesis.html.
[32] F.D. Murnaghan, Proc. Natl. Acad. Sci. U.S.A. 30 (1944) 244.
[33] C. Jiang, Z. Lin, Y. Zhao, Phys. Rev. Lett. 103 (2009) 185501-1.
[34] M.J. Mehl, Phys. Rev. B 47 (1993) 2493.
[35] S.Q. Wang, H.Q. Ye, Phys. Stat. Sol. B 240 (2003) 45.
[36] E. Deligöz, K. Çolakoğlu, Y.Ö. Çiftçi, H. Özışık, J. Phys.: Condens. Matter 19 (2007) 436204 (11 pp.).
[37] C. Zener, Elasticity and Anelasticity in Metals, University of Chicago Press, Chicago, 1948.
[38] B. Mayer, H. Anton, E. Bott, M. Methfessel, J. Sticht, J. Haris, P.C. Schmidt, Intermetallics 11 (2003) 23.
[39] H. Fu, D. Li, F. Peng, T. Gao, X. Cheng, Comput. Mater. Sci. 44 (2008) 774.
[40] J. Haines, J.M. Leger, G. Bocquillon, Ann. Rev. Mater. Res. 31 (2001) 1.
[41] A.F. Young, C. Sanloup, E. Gregoryanz, S. Scandolo, R.E. Hemley, H.K. Mao, Phys. Rev. Lett. 96 (2006) 155501.
[42] S.F. Pugh, Phil. Mag. 45 (1954) 833.
[43] I.R. Shein, A.L. Ivanovskii, J. Phys.: Condens. Matter 20 (2008) 415218.
[44] C. Dong, X. Guo-Liang, Z. Xin-Wei, Z. Ying-Lu, Y. Ben-Hai, S. De-Heng, Chin. Phys. Lett. (2008) 2950.
[45] I. Suzuki, J. Phys. Earth 23 (1975) 145.
[46] Y. Wang, J. Zhang, L.L. Daemen, Z. Lin, Y. Zhao, Phys. Rev. B 78 (2008) 224106-1.